Solar Energy Vol. 34, No. 4/5, pp. 389–405, 1985
Printed in the U.S.A.

0038–092x/85 $3.00 + .00
Pergamon Press Ltd.

SYSTEM MODELING AND OPERATION CHARACTERISTICS OF THERMOSYPHON SOLAR WATER HEATERS

G. L. MORRISON† and J. E. BRAUN
Solar Energy Laboratory, University of Wisconsin-Madison, Madison, WI 53706

(*Received* 23 *January* 1984; *revision received* 7 *November* 1984; *accepted* 7 *November* 1984)

Abstract—An efficient numerical simulation model for thermosyphon solar water heaters has been developed and compared with test data from two locations. The model was used to study the characteristics of vertical and horizontal tank thermosyphon systems. The results indicate that thermosyphon systems have optimum performance when the daily collector volume flow is approximately equal to the daily load volume. Heat conduction in one tank horizontal system was found to significantly reduce solar contribution.

1. INTRODUCTION

Thermosyphon solar water heaters have been widely used in all climates where extended freeze protection is not required. Most thermosyphon designs have been developed by trial and error, since the complexity of varying collector flow rate and a thermally stratified storage tank mean that the well-established design methods for active systems cannot be applied.

There have been many analytic and numerical studies of thermosyphon system performance[1–6]. However, most models are so complex that they have been used only to study performance over a few days or for simplified operating conditions such as no daytime load. There is also very little data on the comparative performance of thermosyphon and active systems. A recent experimental study[14] reported that a thermosyphon system had better performance than five active systems that were tested in parallel. However, simulation studies[16, 23] of active and thermosyphon systems have shown that active systems may perform better than thermosyphon systems if both systems are operated with stratified storage tanks. In addition to a lack of data on the relative performance of thermosyphon and active systems, the effect of design variables such as collector flow rate, one or two tank design, and horizontal or vertical tank configuration have not been studied, even though systems incorporating these features are readily available.

The uncertainty associated withh thermosyphon system design and the complexity of current simulation models prompted the development of a more efficient model. This model was written for the widely used TRNSYS[9] simulation program, and has been used to investigate the design and performance of thermosyphon systems.

2. THERMALLY STRATIFIED STORAGE TANK MODELS

The temperature distribution in the storage tank of a thermosyphon system has a major effect on both the collector inlet temperature and flow rate. At low collector flow rates, a thermosyphon tank exhibits a large degree of stratification.

Most studies[2–6] have used finite difference techniques to simulate the tank temperature stratification. The tank is divided into a series of fixed size nodes, and the variation of temperature with time is computed using an energy balance on each tank node. The energy balance on a stationary control volume of a storage tank includes the enthalpies of the fluid entering and leaving, conduction between adjacent segments and heat loss from the outer surface. The degree of mixing between incoming fluid and the contents of the tank (and therefore stratification) depends upon the number of segments that are utilized. At low flows, there is very little mixing, and a large number of nodes may be required to predict the degree of stratification. Simulations of thermosyphon solar preheat tanks have usually been performed with 10 to 15 nodes[3, 5], while simulations of one tank systems required 20 nodes for vertical tanks and 30 nodes for horizontal tanks[6]. A detailed study of the short-term characteristics of a horizontal tank thermosyphon system[7] required 100 tank nodes to obtain reliable data on the interaction of the solar and auxiliary inputs. As the number of nodes is increased, the solution time step must be reduced to maintain satisfactory numerical accuracy. For a 20-node tank model, simulation time steps of less than five minutes may be required[6].

An alternative modeling approach that is particularly appropriate at low flow rates is to assume

† Permanent address: School of Mechanical and Industrial Engineering, University of New South Wales, Box 1 Kensington, Australia 2033.

that there is no mixing between the incoming flow and fluid in the tank. Energy balances are formulated for moving segments of fluid such that the convection terms do not appear. The advantage of this technique is that the components of the fixed node energy balance equation that have long time constants (heat loss and conduction) are separated from the components that may have short time constants (convection due to collector and load flow). The energy balance equation that includes only heat loss and conduction can then be readily solved with time steps up to one hour, without the numerical accuracy problems that may be present when there is a convection term in the energy balance equation. Convection is then analyzed by a record keeping process on segments of fluid passing in and out of the tank. This plug flow analysis is very similar to the extended SOLSYS model[8] with the following improvements: (i) conduction within the fluid; (ii) optional in-tank auxiliary, subject to temperature and/or time control; (iii) vertical or horizontal cylindrical tank; and (iv) different insulation thicknesses on the top and sides of a vertical tank or eccentric location of the tank and insulation jacket of a horizontal tank.

3. THERMOSYPHON SYSTEM SIMULATION

A thermosyphon system consisting of a flat-plate collector and a stratified storage tank, operating at steady state conditions, can be analyzed in a manner similar to that of Ong[2, 3]. The system is divided into a number (N) of segments normal to the flow direction and Bernouli's equation for incompressible flow is applied to each segment. For steady state conditions, the pressure drop in any segment is

$$\Delta P = \rho_i g\, h_{fi} + \rho_i g\, H_i \tag{1}$$

where h_{fi} is the friction head drop through an element, and H_i is the vertical height of the element.

Also, the sum of the pressure changes around the loop is zero:

$$\sum_{i=1}^{N} \rho_i h_{fi} = \sum_{i=1}^{N} \rho_i H_i. \tag{2}$$

For each time, interval, the thermosyphon flow rate must uniquely satisfy eqn (2). The density of any node is calculated as a function of the local temperature according to the relation of Close[1]. Evaluation of the temperature distribution and head loss in terms of flow rate is discussed in the following sections.

3.1 *Collector*

the collector thermal performance can be modeled by dividing it into N_c equally sized nodes. On the basis of the Hottel-Whillier equation, the temperature at the midpoint of any collector node k is

$$T_k = T_a + \frac{I_T F_R U_L}{F_R(\tau\alpha)} + \left(T_i - T_a - \frac{I_T F_R U_L}{F_R(\tau\alpha)}\right) \exp\left(-\frac{F' U_L A_c}{\dot{m} C_p}\frac{(k-1/2)}{N_c}\right). \tag{3}$$

The collector parameter $F'U_L$ is calculated from collector test data for $F_R U_L$ at the test flow rate $\dot{m}_T$:

$$F'U_L = \frac{-\dot{m}_T C_p}{A_c} \ln\left(1 - \frac{F_R U_L A_c}{\dot{m}_{T_p}}\right). \tag{4}$$

This procedure neglects changes in F' and U_L with flow rate and the dependence of U_L on temperature. The parameter $F_R(\tau\alpha)$ is determined from the intercept efficiency at normal incidence and separate incidence angle modifiers for beam, diffuse and ground radiation[11].

The overall useful energy from the collector is

$$\dot{Q}_U = rA_c[F_R(\tau\alpha)I_T - F_R U_L(T_i - T_a)], \tag{5}$$

where

$$r = \frac{F_R(\dot{m})}{F_R(\dot{m}_T)} = \frac{\dot{m}(1 - e^{-F'U_L A_c/\dot{m}C_p})}{\dot{m}_T(1 - e^{-F'U_L A_c/\dot{m}_T C_p})}.$$

3.2 *Connecting pipes*

The temperature drop along the pipes between the tank and collector is usually small, and the pipes can be modeled as single nodes with negligible thermal capacitance. The average and outlet temperatures are given by

$$T_p = T_a + (T_{pi} - T_a)\frac{\dot{m}C_p}{(UA)_p}(1 - e^{-(UA)_p/\dot{m}C_p}), \tag{6}$$

$$T_{po} = T_a + (T_{pi} - T_a)e^{-(UA)_p/\dot{m}C_p}. \tag{7}$$

3.3 *Tank*

The solution sequence for the tank is illustrated in Fig. 1. In this example, the tank is initially represented by three fluid segments. The first stage of the analysis is to solve for the change of tank segment temperatures due to heat loss to the surroundings and conduction between segments. The energy input from the collector is determined by considering a constant temperature plug of fluid of volume $V_h(=\dot{m}\,\Delta t/\rho)$ entering the tank during the time step Δt. The plug of fluid is positioned in relation to the existing fluid segments using one of the following convection models.

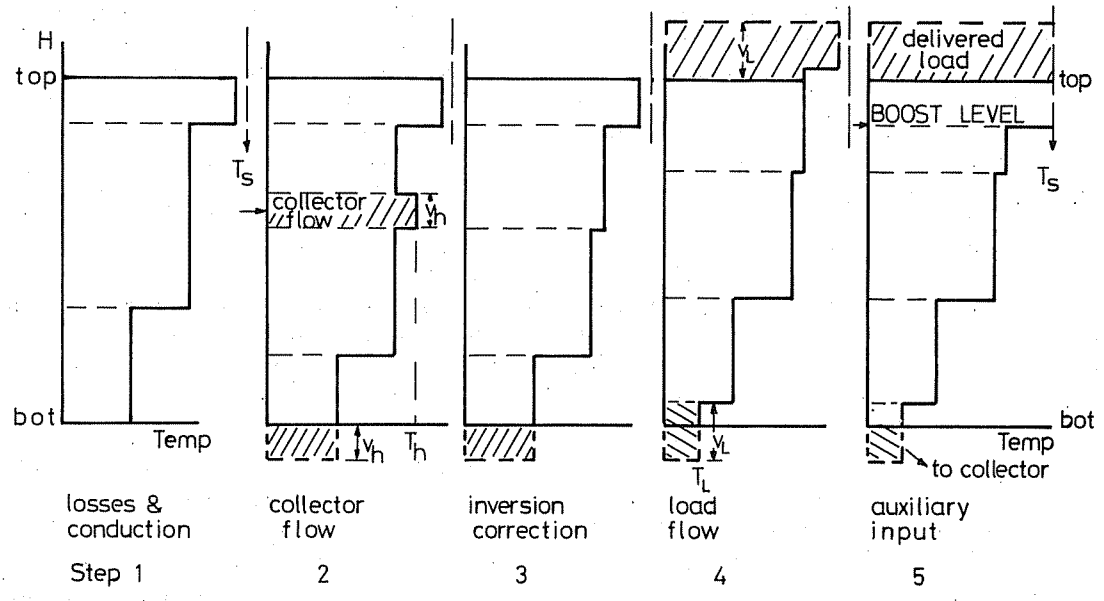

Fig. 1. Algebraic tank model solution sequence.

(a) *Fixed inlet convection model.* The plug of fluid of volume V_h and temperature T_h is initially inserted into the tank below the physical position of the inlet. Segments below this point are moved down the tank by an amount equal to the collector volume flow during the time step (step 2 of Fig. 1). If a temperature inversion is produced by this process, the new segment of fluid is mixed with segments above or below until the inversion is removed (step 3 of Fig. 1).

(b) *Fully stratified convection model.* The plug of fluid entering the tank is placed between existing segments chosen so as to avoid developing a temperature inversion. This model produces the maximum degree of stratification possible.

The load flow is considered in terms of another segment of fluid of volume $V_L(=\dot{m}_L \Delta t/\rho)$ and temperature T_L added either to the bottom of the tank (fixed inlet convection model) or at its appropriate temperature level (fully stratified model). Fluid segments are moved up the tank as a result of the addition of the new load flow segment. The net shift of the profile in the tank above the collector return level is equal to the load volume V_L, and below the collector return is equal to the difference between the collector and load volumes $(V_h - V_L)$ (step 4, Fig. 1). After adjusting for the load flow, the auxiliary input is considered, and if sufficient energy is available, segments above the auxiliary input level are heated to the set temperature (step 5, Fig. 1). If necessary, the segment containing the auxiliary element is split so that only segments of the tank above the element are heated.

Segments and fractions of segments in the new tank profile that are outside the bounds of the tank are returned to the collector and load (step 5, Fig. 1). The average temperature of the fluid delivered to the load is

$$T_d = \sum_{i=1}^{j-1} \frac{(T_i V_i + a T_j V_j)}{V_L}, \tag{8}$$

where a and j must satisfy

$$V_L = \sum_{i=1}^{j-1} (V_i) + a V_j$$

and

$$0 \le a < 1.$$

The average temperature of fluid returned to the collector is

$$T_R = \sum_{i=N_T}^{N_r-l} \frac{(T_i V_i + b T_l V_l)}{V_h}, \tag{9}$$

where l and b must satisfy

$$V_R = \sum_{i=N_T}^{N_r-l} (V_i) + b V_l$$

and

$$0 \le b < 1.$$

The primary advantage of this tank model is that small fluid segments are introduced when stratification is developing, while zones of uniform temperature, such as above the auxiliary heater, are represented by large fluid segments. The size of fluid segments used to represent the tank temperature stratification varies with collector flow rate.

If the collector flow rate is high, there will be little stratification in the preheat portion of the tank, and the algebraic model will produce only a few tank segments. However, if the collector flow rate is low and the tank stratified, then small tank segments will be generated. The size of the tank segments will also decrease as the simulation time step is reduced. To avoid generating an excessive number of segments, adjacent segments are amalgamated if they have a temperature difference of less than 0.5°C. The concept of variable size segments could also be used in the fixed node model, but it would require that the user specify a strategy governing the size and location of the nodes before the simulation is run.

3.4 *Thermosyphon circuit friction*

The friction pressure drop along the connecting pipes is evaluated from the laminar friction factor with allowance for the extra friction due to developing flow in the entrance region of each pipe[10, 12]. If the pipe Reynolds number evaluated at the local temperature is greater than 2000, the friction factor (corrected for developing flow) is evaluated at a Reynolds number of 2000.

The pressure drop across the collector is evaluated theoretically, assuming equal flow distribution between the risers, or if a check valve is used to control reverse thermosyphoning, experimental data for the collector and check valve pressure drop versus flow rate is used. The pressure drop through the storage tank is assumed to be negligible except for minor losses at the entry and exits of the connecting pipes.

3.5 *Solution procedure*

The first step of the solution is to evaluate the temperature distribution around the thermosyphon loop for the flow rate of the previous time step. The inlet temperature to the collector is computed from the bulk mean temperature of the segments in the bottom of the tank with a volume equal to the collector volume flow [eqn (9)]. After allowance for heat loss from the inlet pipe [eqn (6)], the temperature of each of the N_c fixed nodes used to represent the collector temperature profile is evaluated from eqn (3). The temperature of the new fluid segment returned to the tank is computed from the collector outlet temperature and the temperature drop across the return pipe to the tank. A new tank temperature profile is then evaluated.

The thermosyphon pressure head due to density differences around the loop is determined from the system temperature profile. The difference between the friction pressure drop around the circuit and the net thermosyphon pressure is evaluated for this flow rate and for a second flow rate. The two pairs of values of flow rate and net difference between the friction and static pressures are then used to estimate a new flow. The process is repeated until a flow rate that satisfies eqn (2) is found.

Although the correspondence between the modeled tank temperature profile and the profile in a real tank will improve as the time step is reduced, there is very little effect of simulation time step on the computed monthly average solar fraction. For the systems studied in this project, there was only a 1–2% change in monthly solar fraction when the time step was varied from 1 h to 0.1 h. Since time steps of up to 1 h can be used in most cases, the execution time of the plug flow tank model is more than an order of magnitude less than the execution time for a fixed node model.

4. COMPARISON OF THE THERMOSYPHON MODEL WITH EXPERIMENTAL DATA

Two sets of experimental data have been used to test the thermosyphon model. Simulation of a system operating with low collector flow rates was compared with the measured performance of a system tested at the National Bureau of Standards, Gaithersburg, Maryland, U.S.A.[13, 14]. Simulation results for systems operating with high collector flow rates for both vertical and horizontal tanks were compared with data reported by the University of New South Wales in Sydney, Australia[15].

4.1 *National Bureau of Standards thermosyphon test data*

As well as monitoring the monthly average performance over a year[13, 14], the National Bureau of Standards also measured collector and tank temperatures and thermosyphon flow rate for a short period in 1982[16]. The system consisted of three collectors mounted in parallel, 4.2 m^2 aperture area, 30 parallel 4.93 mm risers, $F_R(\tau\alpha)_n = 0.805$ $F_R U_L = 4.73$ W/°C m^2, $K_{\tau\alpha} = 1.0 - 0.1\,(1/\cos\theta - 1)$. It should be noted that the thermal performance measurements for the collector were obtained using a mass flow rate of 0.02 kg/s m^2. The collectors were connected to a 0.242 m^2 storage tank ($UA = 1.47$ W/°C) by 25 mm ID pipes (Fig. 2), with a check valve to prevent reverse thermosyphon flow. The pressure drop data for the collector and check valve are shown in Fig. 3. Two sets of data on the system performance and environmental conditions, measured at 10-minute invervals, have been used to check the thermosyphon model. The data recorded on 17 December 1982 included collector and tank temperatures, and the thermosyphon flow rate was measured with an *in situ* calibrated thermistor anemometer[16]. During this test, the auxiliary heater was not activated, and a single load of 52 l was applied at noon. For both the tests outlined here, the collector flow was returned to the top of the tank.

During another test, the daily system performance was measured from Jan.–Dec. 1980, while a

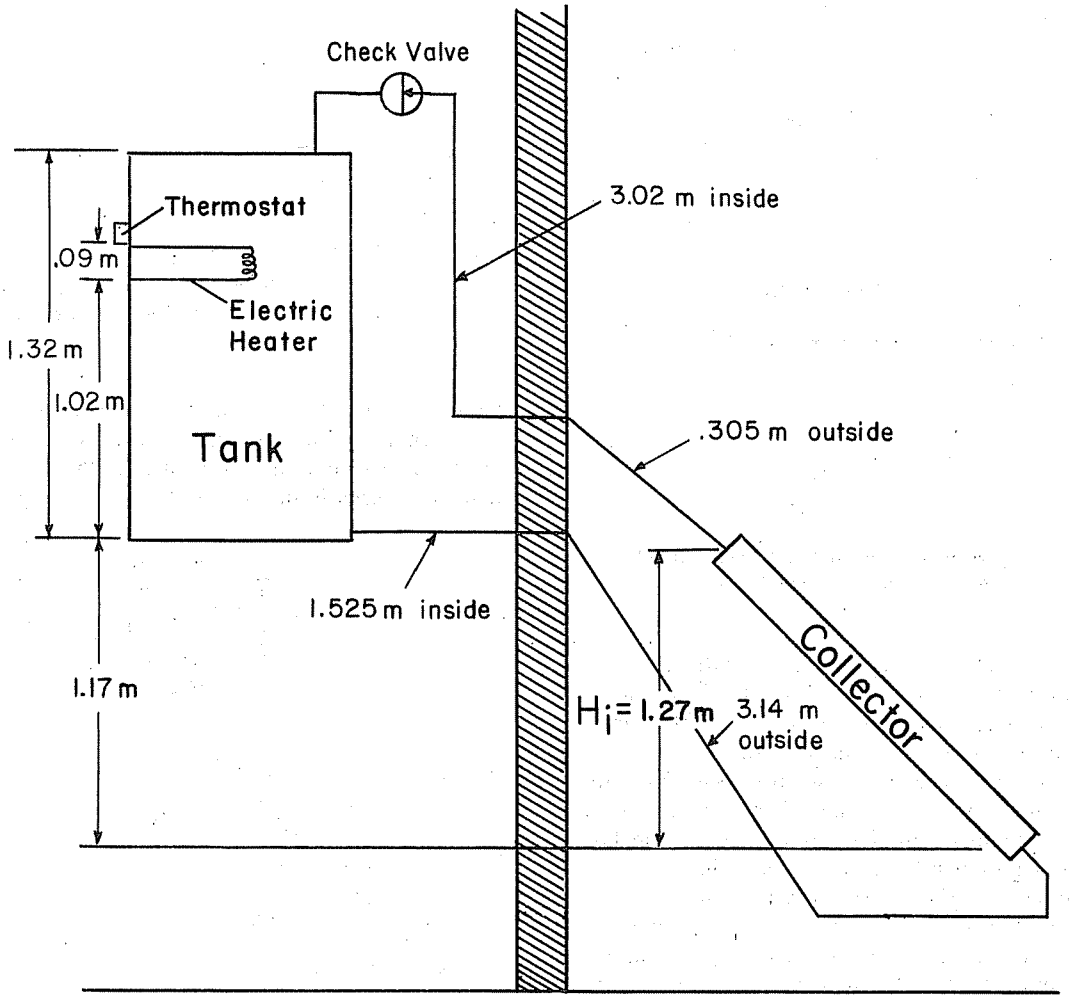

Fig. 2. Thermosyphon system tested at National Bureau of Standards, Gaithersburg, Maryland, U.S.A.

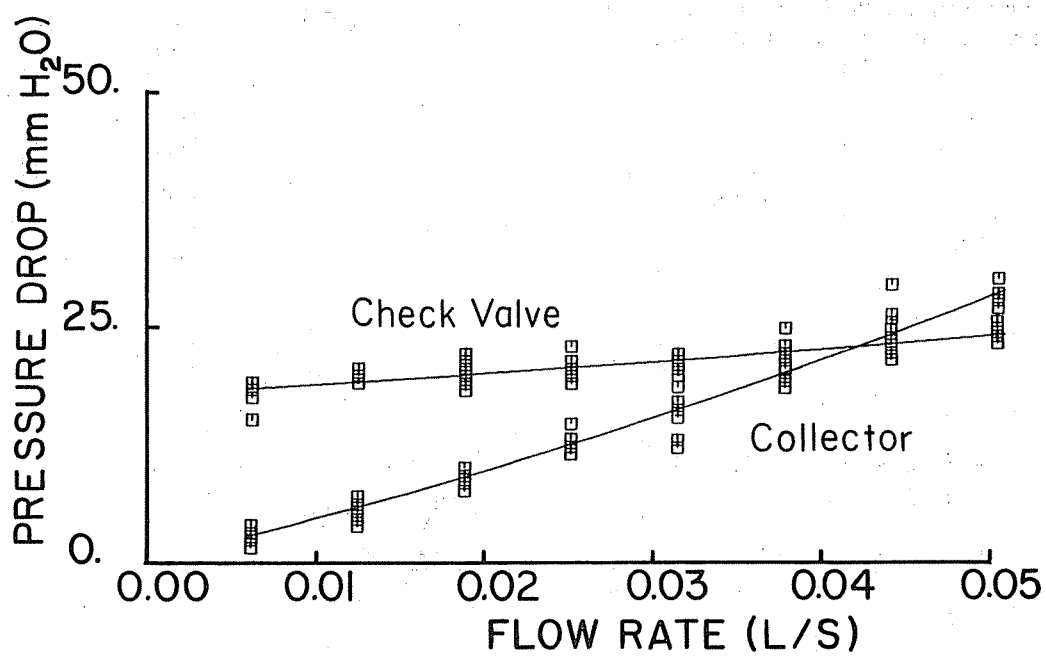

Fig. 3. Collector and check valve pressure drops for system tested at National Bureau of Standards.

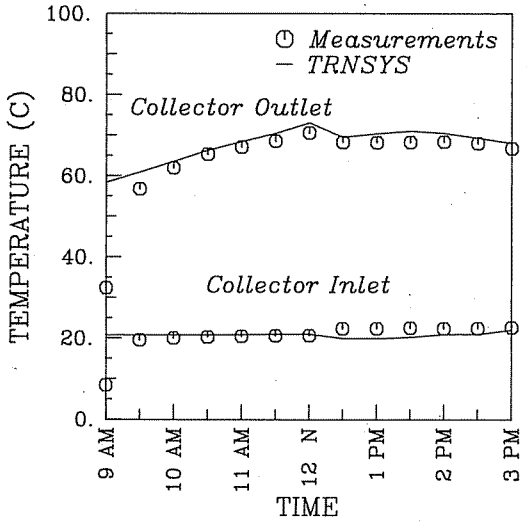

Fig. 4. Comparison of measured and predicted collector inlet and outlet temperatures.

daily load of 250 l was withdrawn with the Rand distribution[17]. The heater (Fig. 2) was activated, and controlled by a thermostat with a set temperature of 63°C and a 14°C deadband.

The measured and simulated results for collector and tank temperatures and thermosyphon flow rates are compared in Figs 4–6. For most of the day, the simulation results for the collector inlet and outlet temperature (Fig. 4) compare favorably with the measured performance. However, at the beginning of the day, there is a large error. The simulation does not account for thermal capacitance in the collector and piping, and thus, the simulated collector reacts instantaneously to the solar input. Although there is a large error in the predicted collector temperature rise, the flow rate during this time of day is low, and hence the net effect on the daily energy

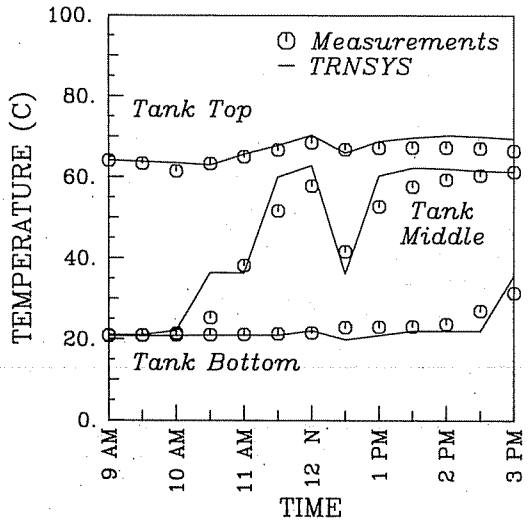

Fig. 5. Comparison of measured and predicted tank temperatures.

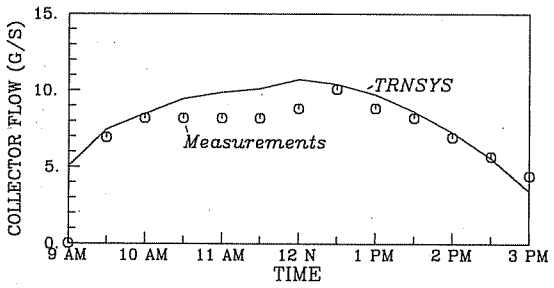

Fig. 6. Comparison of measured and predicted thermosyphon flow rate.

collection is small. The predicted and measured tank temperatures (Fig. 5) also show reasonable agreement. The discontinuous nature of the predicted temperatures is due to the finite fluid seg-

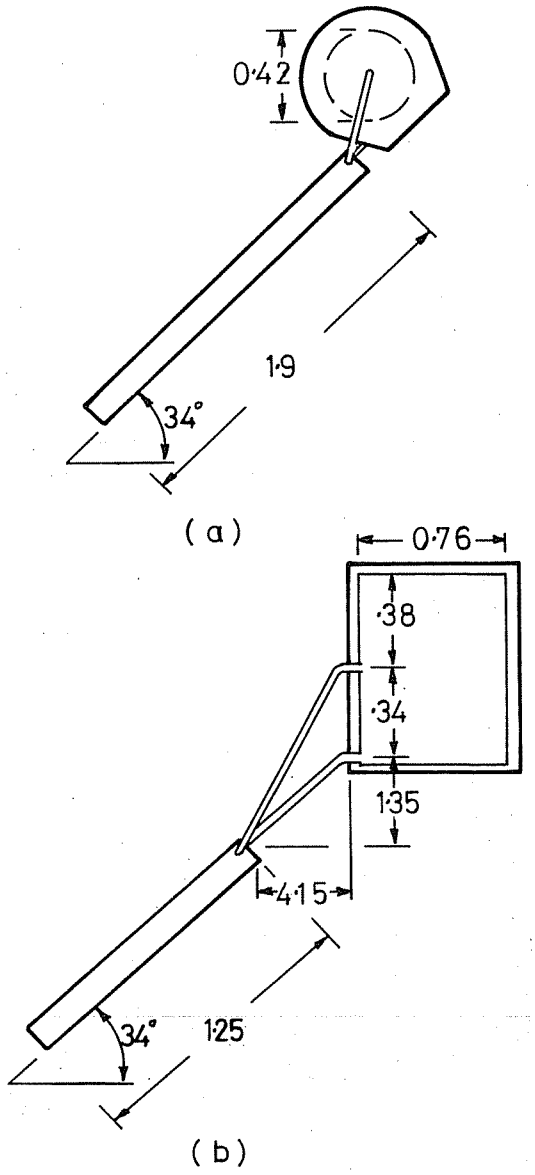

Fig. 7. Thermosyphon system configurations tested in Sydney, Australia. (a) horizontal tank, (b) vertical tank.

Table 1. Comparison of experimental and simulation results for thermosyphon systems tested at National Bureau of Standards, Gaithersburg, Maryland, U.S.A.

Date 1980	Measured Load MJ/day	Measured Auxiliary MJ/day	f_r*	Simulation Load MJ/day	Simulation Auxiliary MJ/day	f_r*
Jan	907	630	0.43	929	655	0.42
Feb	1095	446	0.65	1096	510	0.63
Mar	1530	796	0.55	1514	883	0.52
Apr	990	284	0.75	946	278	0.76
May	1164	403	0.71	1195	423	0.71
June	1099	299	0.77	1165	312	0.79
July	913	198	0.82	896	164	0.85
Aug	604	216	0.72	617	226	0.71
Sep	950	270	0.78	978	218	0.83
Oct	781	382	0.61	792	314	0.68
Nov	1670	1033	0.46	1590	969	0.5
Dec	483	265	0.54	471	264	0.53
Annual	12187	5222	0.65	12188	5219	0.65

f_r* = fractional energy savings relative to conventional system with tank loss of 11.6 MJ/day (13, 14)

ments that are used to represent the tank temperature stratification. The measured and predicted thermosyphon flow rates (Fig. 6) agree within the ±10% uncertainty of the thermistor anemometer[16].

Results of the annual comparison of measured and predicted performance, when the system was operated with auxiliary heating, are given in Table 1. Good agreement between the simulation and measurements was found for both delivered load and auxiliary consumption. For both sets of tests the simulation results were almost identical for both the fully stratified and fixed inlet convection models. The ratio of total collector volume flow to total load volume during these tests was 0.8 to 0.9. In Sec. 7 of this paper, the ratio of total collector volume flow to total load volume is shown to be a major factor effecting system performance.

4.2 *Australian thermosyphon test data*

Details of two common Australian thermosyphon designs that were tested during 1981/1982 in Sydney, Australia[15] are given in Fig. 7. These systems were designed to operate with high collector flow rate so that the fluid temperature rise is limited to 10 to 15°C per pass through the collector. As well as monitoring the monthly average performance, detailed measurements of the tank temperature profile were also made on one system while typical domestic loads were applied.

Comparison of the thermosyphon model predictions and the measured performance of four systems operating in Sydney, Australia, is shown in Figs 8 and 9 for a vertical tank system with continuous and nighttime (2000 to 600 h) auxiliary input, and in Figs 10 and 11 for a horizontal tank. The tests in 1982 used loads 25 to 30% higher than the tests in 1981; details of loads, delivery temperatures and system performance are given in Refs. [6] and [15]. The agreement between predicted and actual performance is generally quite good. There is little difference between the two convection models for the systems operated with nighttime only auxiliary input. The difference between the models is greater when the auxiliary input is continuously available (thermostat control) but is reduced when the test loads are increased.

Conduction between the auxiliary and preheat

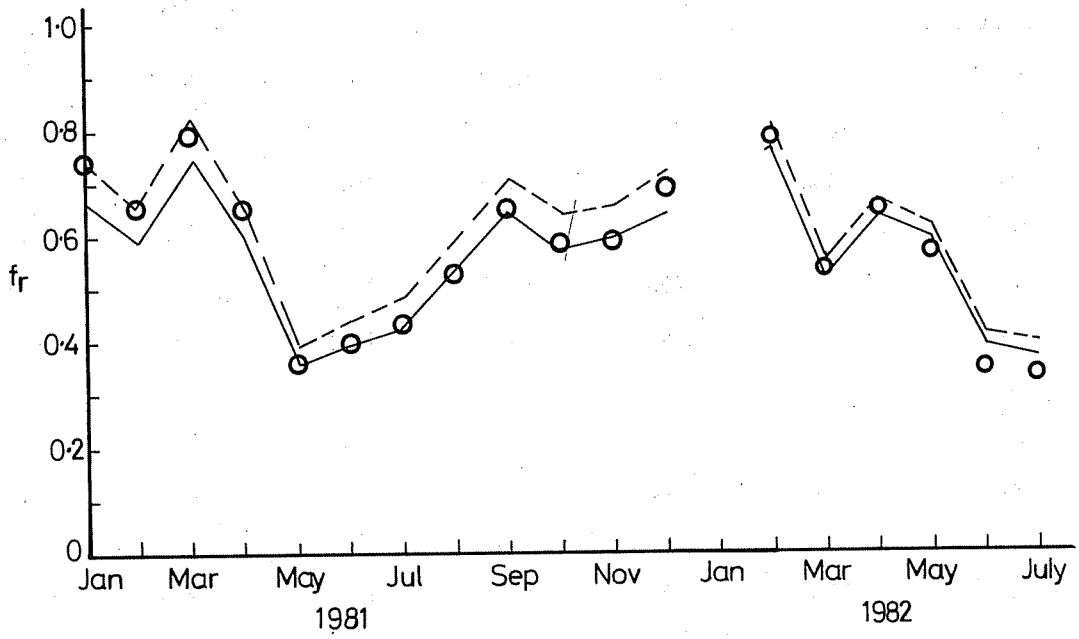

Fig. 8. Observed and predicted solar contribution. Vertical tank (H/D = 1) thermosyphhon system with continuous electric boost. O, observed performance; – – –, fully stratified simulation; ——, fixed inlet simulation.

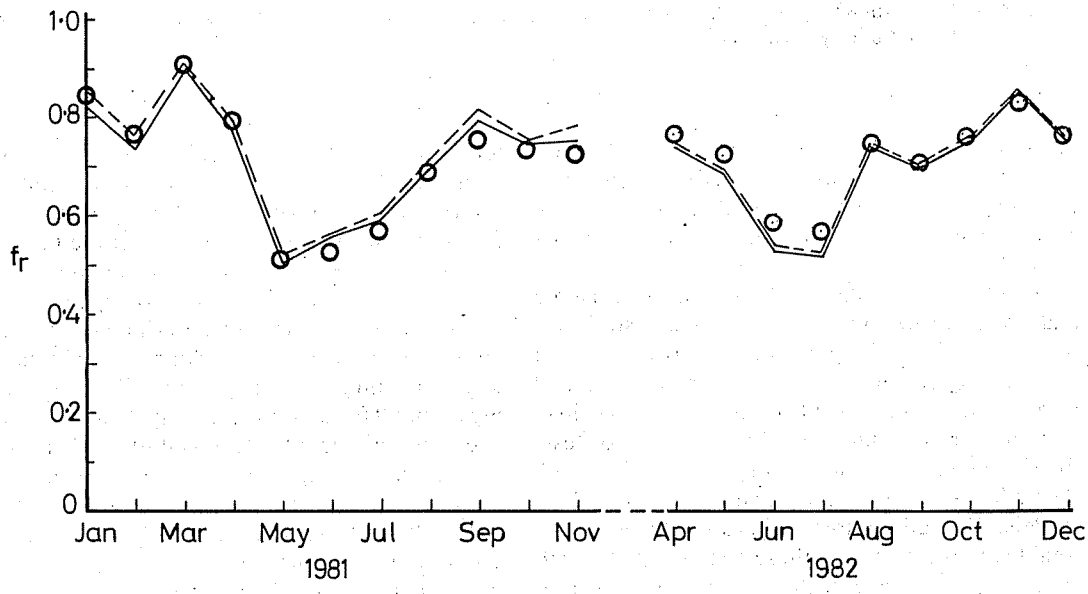

Fig. 9. Observed and predicted solar contribution. Vertical tank (H/D = 1) thermosyphon system with night time only boost. O, observed performance; – – –, fully stratified simulation;——, fixed inlet simulation.

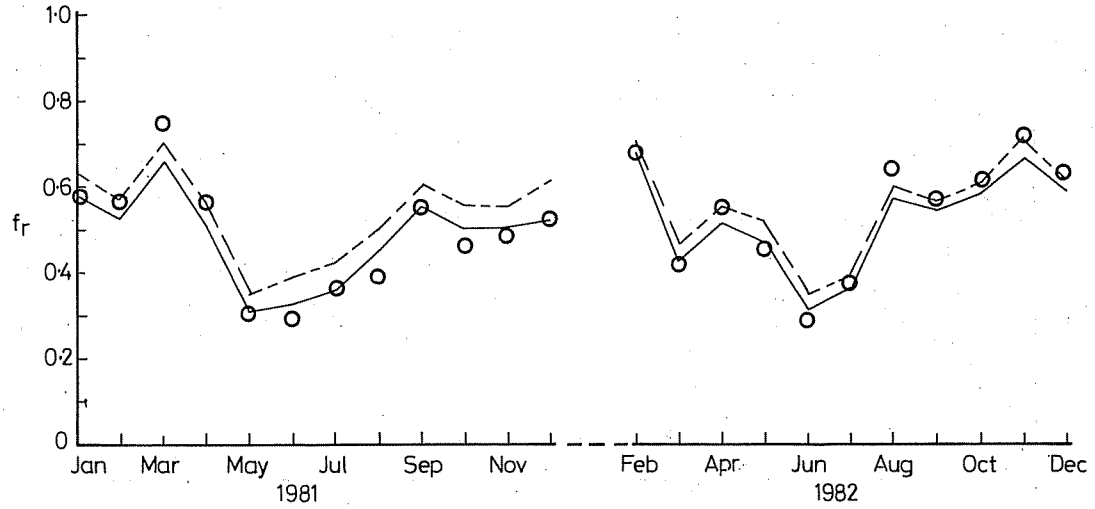

Fig. 10. Observed and predicted solar contribution. Horizontal tank thermosyphon system with continuous electric boost. O, observed performance; – – –, fully stratified simulation; ——, fixed inlet simulation.

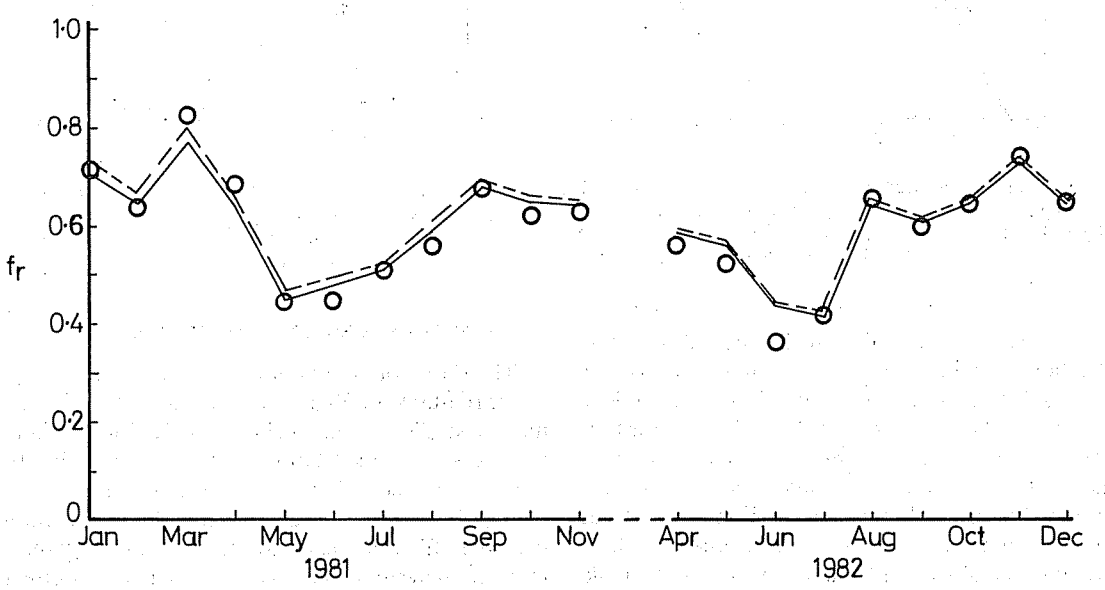

Fig. 11. Observed and predicted solar contribution. Horizontal tank thermosyphon system with night time only boost. O, observed performance; – – –, fully stratified simulation; ——, fixed inlet simulation.

sections of a single-tank heater is more significant when auxiliary is operated continuously. The difference between the results of the two convection models for these systems is primarily due to differences in predicted conduction between these two zones. The fully stratified model predicts more stratification and therefore less auxiliary conduction to the preheat zone as compared with the fixed inlet model. This results in lower collector inlet temperatures and greater collection. Higher load flows tend to remove the effects of conduction between the auxiliary and preheat sections, so that both convection models yield similar results. It is difficult to conclude from the comparisons which model is most appropriate. Both convection models yield results that are within the accuracy of the experiments.

The tank temperature profile in the vertical tank system with continuously available auxiliary input is compared with the step-wise simulated tank temperature profile in Figs 12 and 13. During the first day of comparison (Fig. 12), there was very little solar input, and the computed daily total collector volume flow was 150 l and the load volume was 166 l. The main period of collector flow was 1000 to 1200 h, but the collector outlet temperature was low. As a result, the stratification in the bottom portion of the tank was disturbed at 1200 h. By 1500 h, conduction from the top section of the tank had reestablished the smooth temperature gradient in

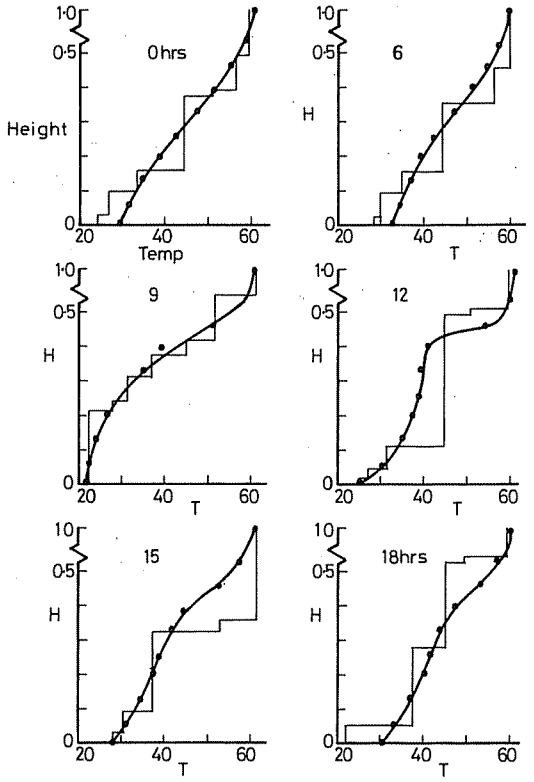

Fig. 12. Tank temperature profile, 4-April-82. ● measured; —— algebraic tank thermosyphon model, for system in Figure 7B. Total irradiation = 4 MJ/m²day, total collector flow = 150 l/day (simulation).

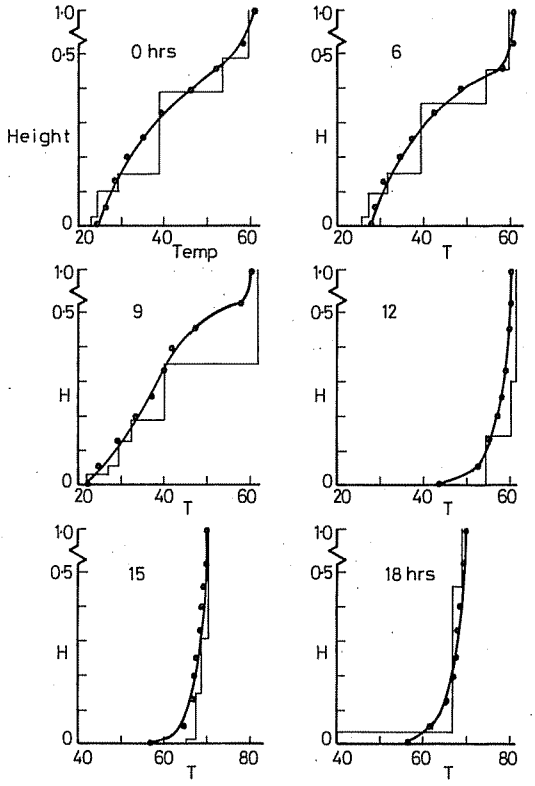

Fig. 13. Tank temperature profile, 5-April-82. ● measured; —— algebraic tank thermosyphon model, for system in Figure 7b. Total irradiation = 26 MJ/m²day, total collector flow = 770 l/day (simulation).

the midzone of the tank. On the second day (Fig. 13), the solar input was very high, and the computed daily collector volume flow was 770 l and the load flow was 158 l. As a result of the high collector flow rate and heat input, the tank was well mixed by the end of the day, and the auxiliary element was not activated after 900 h. The comparison of measured and simulated tank temperature profiles on these two extreme days is reasonable in most of the tank, except for the middle zone where the auxiliary element is located. This is due to differences in the thermostat switching time between the model and real system.

5. EFFECT OF CONDUCTION IN STRATIFIED TANKS

The effect of conduction on the performance of the three-tank configurations used in the experimental studies is shown in Table 2. Each system has the same tank UA (3.9 W/°C), volume (300 l), auxiliary heated volume (135 l) and set temperature (60°C). The results in Table 2 show that conduction has little effect on the performance of tall tank thermosyphon systems but has a very significant effect on the performance of horizontal tank systems. The performances of the three systems differ when conduction is not considered because of differences in the surface area of the auxiliary controlled volume.

Table 2. Effect of conduction on system performance

Tank Type	H/D or L/D	Solar Fraction	
		conduction	no conduction
Vertical	2.7	77.4	79.2
Vertical	1	73.8	79.3
Horizontal	5.3	68.9	79.0

January Only

Table 3. Effect of using separate auxiliary tank in horizontal tank thermosyphon system

Month	Solar Contribution f_R One-Tank System	Two-Tank System
Jan. 82	57.8	61.8
Feb.	67.2	68.9
Mar.	43.3	49.5
Apr.	51.5	57.0
May	47.3	54.9
June	32.0	41.1
Jul.	32.0	40.1
Aug.	51.0	57.1
Sep.	47.8	53.9
Oct.	52.2	57.2
Nov.	60.2	63.8
Dec.	50.9	56.1
Annual	48.6	54.5

The loss of performance due to conduction is primarily caused by heat conduction from the top auxiliary zone into the preheat zone. The short conduction path in horizontal tanks results in significant heating of the preheat zone. Thus, maximum stratification cannot be maintained in horizontal tanks, even if low collector flow rates are used. Most of the heat conduction out of the auxiliary zone in tall tanks is carried back up the tank by the load flow before it can affect the collector inlet temperature. The effect of conduction in horizontal tanks is also reduced for larger loads.

6. TWO-TANK THERMOSYPHON SYSTEMS

The influence of conduction on the performance of horizontal tank systems can be reduced by using a separate auxiliary tank to eliminate the conduction between the auxiliary and preheat zones. To avoid the increased tank heat loss that is a result of the larger surface area, the two tanks could be mounted end to end. The performance of one- and two-tank horizontal systems, with the same total tank UA, is shown in Table 3. The annual solar contribution (F_r) increased from 0.49 for the one-tank system to 0.55 for the two-tank system for a system operating with loads of 30 MJ/d in summer and 38 MJ/d in winter. The change of performance for vertical tank systems would be less than for horizontal tank systems, since conduction is not as important. However, a baffle between the auxiliary and preheat zones in a squat vertical system would improve the system performance.

7. EFFECT OF COLLECTOR FLOW RATE ON SYSTEM PERFORMANCE

The benefit of using a thermally stratified storage tank has been well documented for active solar systems[18–22]. By using low collector flow rates to promote stratification, the collector inlet temperature can be held much lower than for a mixed tank. However, there is a tradeoff between the benefit of lower collector inlet temperature and a loss of performance due to lower collector flow rates.

Braun and Fanney[16] have shown that the effect of collector flow rate on the long-term performance of thermosyphon (and active) systems can be correlated in terms of the ratio of total volume flow through the collector to total load volume (M_c/M_L). This factor is used to correlate the variable flow rate simulation results in this study.

The effect of collector flow rate on thermosyphon system operation is shown in Fig. 14 for two

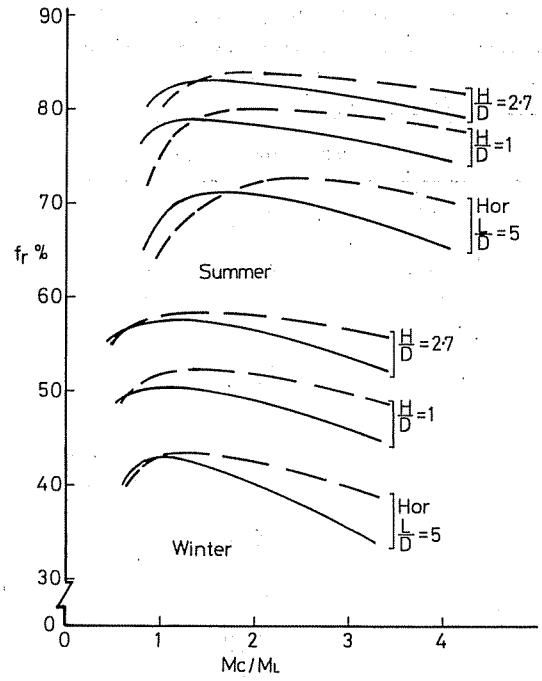

Fig. 14. Solar fraction as a function of collector to load flow ratio. Vertical tanks H/D = 2.7, 1. Horizontal tank L/D = 5. Same collector and tank UA for each case. -- – Fully stratified model, —— Fixed inlet model.

vertical tank systems and one horizontal tank system with the same tank volume (300 l), UA (3.9 W/°C) and collector array (4 m^2, $F_R(\tau\alpha)$ = 0.65, $F_R U_L$ = 4.5 W/°C – m^2). The simulation results for the fully stratified tank model are higher than for the fixed inlet model for high collector flow rates, due to the lower collector inlet temperature that is produced by the assumption of maximum stratification. However, at low collector flow rates, the relative predictions of the two models reverse. The fully stratified model produces a layer of very hot fluid at the top of the tank, and as a result, the tank heat losses are higher than for the partial stratification predicted by the fixed inlet model. Comparison of the measured and simulated results in Figs. 9 and 11 shows that at high collector flow rates, the fixed inlet model gives a better estimate of the long-term performance. For low collector flow rates, however, the National Bureau of Standards results (Table 1) indicate that the fully stratified model gives a slightly better estimate of performance.

The data in Fig. 14 shows that the optimum collector to load volume ratio for a tall tank thermosyphon system varies from 1.0 to 1.2 in summer to 0.8 to 1.0 in winter. Wuestling *et al.*[23] found similar results for tall tank pumped systems and showed that the optimum ratio of collector to load flow was not sensitive to location. For thermosyphon systems, the difference between performance at high collector flow rate and the optimum collector flow is only three percentage points in solar contribution for tall tank systems but up to six percentage points for horizontal tank systems.

Horizontal one-tank systems are more sensitive to collector flow rate than tall tanks. The conduction path between the auxiliary zone and the bottom of the tank is very short in horizontal tanks. Thus, heat conduction from the auxiliary zone reaches the bottom of the tank and influences the collector performance very quickly.

7.1 *Thermosyphon versus pumped circulation*

In an outdoor system test at the National Bureau of Standards[14], a thermosyphon system was found to perform better than five active systems. However, all the pumped systems were operated at high flows such that the preheat tanks were fully mixed. The superior performance of the thermosyphon system could have been due to better stratification in the preheat section.

To compare equivalent active and thermosyphon systems, simulations were performed for one-tank configurations of both types of systems (Fig. 2), when operated with low collector flow rates, subjected to the Rand[17] load profile.

The results in Fig. 15 indicate that there is very little difference in the performance of active and thermosyphon systems at low collector flow rates. At the optimum collector flow rate and for the Rand load profile, the active system performs slightly better than the thermosyphon. However, the relative performance of the two systems changes with load profile, and the controller dead bands used in the active system. For a daytime load profile, the thermosyphon system performs slightly better than the active system but there is very little difference between the performance of the two systems when both are operated with the optimum collector flow rate.

If the pumped system is operated with a conventional high collector flow rate of 50 kg/m^2 h, the

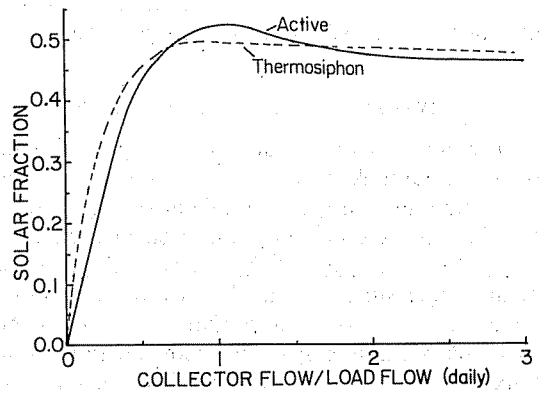

Fig. 15. Comparison of pumped and thermosyphon system performance.

preheat section of the tank will be fully mixed and the annual solar fraction is 0.36 versus 0.5 for the optimum collector flow to load flow ratio.

8. EFFECT OF DAILY LOAD PROFILE ON THERMOSYPHON SYSTEM PERFORMANCE

A thermosyphon system operates with a variable flow that is a function of the meterorological conditions and the temperature distribution in the tank. As the temperature in the tank is increased, the thermal driving forces are reduced. Thus, a load profile that keeps the preheat section of the tank filled with water at cold supply temperature will produce best performance. To achieve this, the instantaneous load flow would need to be greater than or equal to the collector flow. A load profile that peaks in the middle of the day will approximate this optimum load.

The effect of load profile on horizontal and vertical tank systems is shown in Table 4, for the morning, afternoon, nighttime and distributed daytime profiles given in Table 5.

The results in Table 4 show that thermosyphon systems are more sensitive to load profile than the fully mixed tank pumped systems studied by Buckles and Klein[27]. The increased effect of load profile is due to the use of a stratified tank. Low flow

Table 4. Effect of load profile on thermosyphon system performance

Tank Volume = 300 ℓ

Tank	Load Pattern	Load ℓ/Day	Solar Fraction f_R
Vertical H/D = 2.7	morning	150	0.81
	afternoon	150	0.83
	daytime	150	0.84
	night	150	0.81
"	morning	300	0.63
	afternoon	300	0.68
	daytime	300	0.68
	night	300	0.57
Horizontal L/D = 5.3	morning	150	0.75
	afternoon	150	0.75
	daytime	150	0.78
	night	150	0.69
"	morning	300	0.60
	afternoon	300	0.61
	daytime	300	0.64
	night	300	0.48

Table 5. Load profiles (fraction of daily total load)

Time	Morning Load	Afternoon Load	Daytime Load	Night Load
0-7	0	0	0	0
7-8	0.2		0.05	
8-9	0.2		0.075	
9-10	0.2		0.1	
10-11	0.2		0.1	
11-12	0.2	0	0.15	
12-13	0	0.2	0.15	
13-14		0.2	0.15	
14-15		0.2	0.1	
15-16		0.2	0.075	
16-17		0.2	0.05	
17-18		0	0	
18-19				0
19-20				0.2
20-21				0.2
21-22				0.2
22-23				0.2
23-24				0.2

rate pumped systems show similar variation of performance with load profile.

Both vertical and horizontal tank thermosyphon systems perform best when loads are distributed throughout the collector operating period (daytime load profile). In vertical tank systems operating with a collector to load flow ratio near one, there is very littlle difference between the distributed daytime load profile and the afternoon load profile. However, for high load flows there is a significant difference in performance between nighttime and daytime loads. The main reason for the difference is due to lower tank heat loss, as a result of lower nighttime preheat section temperatures, produced by the daytime or afternoon load profiles.

The effect of load profile on horizontal tank systems is different than the effect on vertical tank systems. In horizontal tanks, the penalty introduced by heat conduction through the preheat zone is greatly reduced by daytime loads. Thus, the distributed daytime load profile produces better performance than either the morning or afternoon load profiles. Also, the nighttime load profile introduces a greater penalty for horizontal tanks, since conduction in horizontal tanks in increased by the high daytime tank temperature produced by this profile.

9. THERMOSYPHON OPERATION CHARACTERISTIC

Experimental data on the instantaneous collector temperature rise in thermosyphon systems[1, 5, 16, 24] indicate that, on clear days, thermosyphon

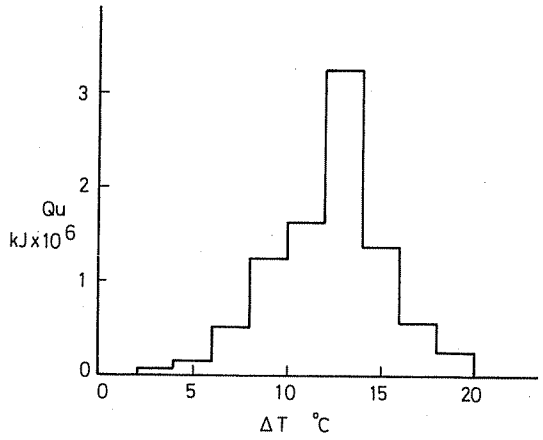

Fig. 16. Collector output versus temperature rise across thermosyphon circuit. Annual collector to load flow ratio = 3.3. Vertical tank H/D = 1.

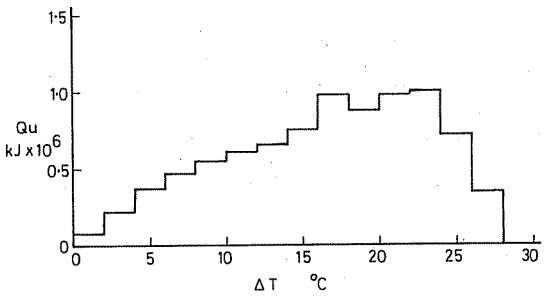

Fig. 17. Collector output versus temperature rise across the collector; pumped circulation. Annual collector to load flow = 3.2. Vertical tank H/D = 1.

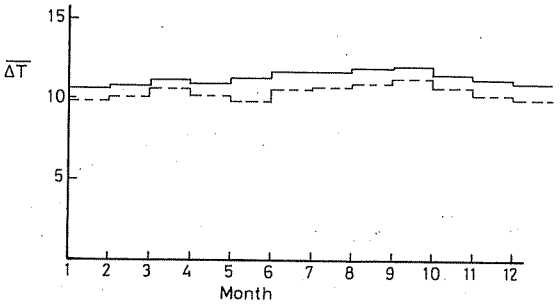

Fig. 18. Monthly average temperature rise across the collector circuit. —— Vertical tank H/D = 1, M_C/M_L = 4.2 − 2.1. -- Horizontal tank L/D = 5, M_C/M_L = 3.4 − 1.9.

systems operate within a narrow range of collector temperature rise.

The collector temperature rise in the low friction upright tank system shown in Fig. 7(b) is very steady, and the measured value of this temperature difference has been used in a thermosyphon system model to simplify the calculation of thermosyphon flow rate[25, 26]. The advantage of this concept is that the simpler thermosyphon flow model does not require accurate simulation of the tank temperature stratification, since the flow rate is computed from

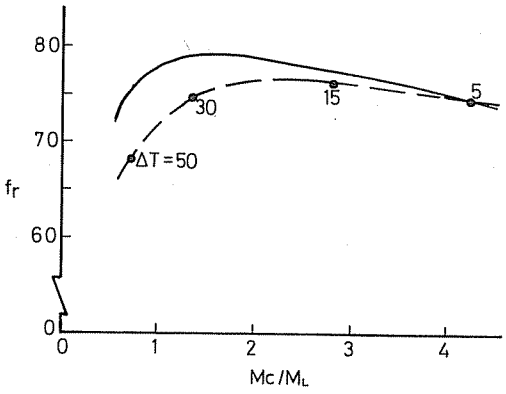

Fig. 19. Solar fraction versus mean collector to load flow. —— Complete simulation. -- Fixed collector temperature rise (ΔT) simulation. Vertical tank H/D = 1.

the specified ΔT and not from a balance of friction pressure drop and thermosyphon driving pressure.

This characteristic of thermosyphon systems was investigated for systems supplying typical domestic loads over a period of a year. A histogram of the collector useful energy versus collector temperature rise is shown in Fig. 16 for a vertical tank system with a low friction resistance thermosyphon loop (annual mean collector volume to load volume = 3.3). The corresponding data for the same tank and collector array operated as a pumped system with the same annual collector volume to load ratio is shown in Fig. 17.

The data in Figs 16 and 17 indicate that the thermosyphon version of this system operates within a much narrower range of values of collector temperature rise than the pumped system. However, the limited range of operating conditions was not as marked for the same system with high friction resistance (lower collector flow rates), or for a low friction resistant horizontal tank system.

Although all thermosyphon systems do not operate with a constant collector temperature rise, the monthly average temperature rise for low friction resistance systems is essentially constant (Fig. 18).

The accuracy of the simplified constant collector temperature rise thermosyphon model can be gauged by the comparison shown in Fig. 19 of the complete system simulation for a range of collector flow rates, with the simulation results obtained from the fixed ΔT model for a range of values of ΔT (which correspond to variations in the collector flow rate). The results in Fig. 19 indicate that the fixed ΔT model of thermosyphon operation can be used to simulate high collector flow rate systems (if ΔT is known) but significantly underestimates the performance of systems operating with low collector flow rates. In addition to the failure to accurately model all possible modes of operation, the major difficulty with the fixed ΔT model is that there is currently no way of calculating ΔT for a given system. Also, the benefit of faster execution time that prompted its development[25, 26] has

been substantially reduced as a result of the new tank model proposed in this paper.

10. CONCLUSIONS

An efficient numerical simulation model for thermosyphon solar water heaters has been developed, and good agreement was found between the simulation results and experimental data for two test locations.

The performance of one-tank thermosyphon solar water heaters is maximized when the daily collector volume flow is approximately equal to the daily load flow. The dependence of performance on collector flow rate (for daily collector volume flow greater than daily load volume) is due to heat conducted between the auxiliary zone and the preheat zone of the tank and convection caused by high collector flow rates.

Horizontal tank systems do not perform as well as vertical tank systems, since the short conduction path in horizontal tanks results in significant heating of the preheat zone. The penalty introduced by a horizontal tank is a function of the daily load volume and load profile.

Daytime load flows reduce the effect of conduction in the preheat zone. For the optimum daily collector to load flow ratio of 1 and daily load volume equal to 50% of the tank volume, the solar fraction of a horizontal tank system is approximately 7% less than an equivalent vertical tank system. For a daily load volume equal to the tank volume, the difference is 6%. The effect of conduction in horizontal tanks can be reduced by using a two-tank system. The improvement in performance of 0.49 to 0.55 solar faction observed in one study should be sufficient to justify the increased cost of a two-tank design, particularly if both tanks are combined end to end in one horizontal package.

Thermosyphon systems show more dependence on daily load profile than high flow rate pumped systems. A load profile with a substantial afternoon component produces best performance in a vertical tank system, while a distributed daytime profile is best for horizontal tank systems.

Thermosyphon and pumped circulation systems have very similar performance if both are operated with a daily collector to load volume ratio of 1. However, thermosyphon systems perform better than high collector flow rate pumped systems due to the advantage of stratification in the thermosyphon tank. Simplified models based on an assumed constant collector temperature rise do not adequately simulate the characteristics of a thermosyphon system.

Acknowledgement—The assistance with the analysis of experimental data given by Dr. A. H. Fanney of the Building Equipment Division of the National Bureau of Standards is gratefully acknowledged.

NOMENCLATURE

- a, b Fractions of a tank segment
- A Tank surface area
- A_c Collector aperture area
- A_p Pipe surface area
- C_p Specific heat
- F' Collector efficiency factor
- F_R Collector heat removal factor
- f Solar contribution to load (load-auxiliary)/load
- f_r Fractional energy savings relative to conventional electric system
- g Acceleration due to gravity
- H_i Vertical height
- h_{fi} Friction pressure head
- I_T Incident irradiation
- $\dot{m}$ Collector flow rate
- $\dot{m}_L$ Load flow rate
- $\dot{m}_T$ Collector flow rate during testing
- M_c Total monthly collector mass flow
- M_L Total monthly load mass flow
- N Number of nodes in the thermosyphon loop
- N_c Number of fixed nodes in the collector
- N_T Number of fluid segments in the tank
- r Flow rate corrector factor
- T_a Ambient temperature
- T_d Temperature of fluid delivered to load
- T_n Temperature of segment returned to the tank
- T_i Collector inlet temperature
- T_k Temperature of node k in collector
- T_L Makeup water temperature
- T_R Average temperature of fluid passing from tank into thermosyphon circuit
- T_s Thermostat set temperature
- U_L Collector heat loss coefficient
- U_p Pipe heat loss coefficient
- V Volume
- V_h Volume of fluid passing through collector during one-time step
- V_L Load volume during one-time step
- $(\tau\alpha)$ Effective transmittance absorptance product
- ρ Density
- ΔT Collector temperature rise
- Δt Simulation time step

REFERENCES

1. D. J. Close, "The Performance of Solar Water Heaters with Natural Circulation". *Solar Energy* **6,** 33–40 (1962).
2. K. S. Ong, "A Finite Difference Method to Evaluate the Thermal Performance of a Solar Water Heater". *Solar Energy* **16,** 137–147 (1974).
3. K. S. Ong, "An Improved Computer Program for the Thermal Performance of A Solar Water Heater". *Solar Energy* **18,** 183–191 (1976).
4. B. Nimmo, W. Clark and J. Pearce, "Analytical and Experimental Study of Thermosyphon Solar Water Heater". *Proceedings of the Annual Meeting of the American Section, ISES*, Orlando, Florida, 4–30, 4–34 (1977).
5. M. F. Young and J. B. Bergguam, "Performance Characteristics of a Thermosyphon Solar Domestic Hot Water System". *ASME J. Solar Energy Engng* **103,** 193–200 (1981).
6. G. L. Morrison and N. H. Tran, "Simulation of the Long-Term Performance of Thermosyphon Solar Water Heaters". *Solar Energy* **33,** 515–526 (1984).
7. S. R. James and D. Proctor, "Development of a Standard for Evaluating the Thermal Performance of a Domestic Solar Hot Water System". *Proceedings of the Annual Conference, ISES, ANZ section, Brisbane, Australia*, 57–65 (1982).

8. J. K. Kuhn, G. F. vanFuchs and A. P. Zob, "Developing and Upgrading of Solar System Thermal Energy Storage Simulation Models". Final Report for U.S. Department of Energy by Boeing Computer Services Co. (1980).
9. S. A. Klein *et al.*, TRNSYS 12.1 User's Manual. University of Wisconsin, Solar Energy Laboratory (1983).
10. G. L. Morrison and D. B. J. Ranatunga, "Transient Response of Thermosyphon Solar Collectors". *Solar Energy* **24,** 55–61 (1980).
11. M. J. Brandemuehl and W. A. Beckman, "Transmission of Diffuse Radiation Through CPC and Flat Plate Collector Glazings". *Solar Energy* **24,** 511–513 (1980).
12. G. L. Morrison and D. B. J. Tanatunga, "Thermosyphon Circulation in Solar Collectors". *Solar Energy* **24,** 191–198 (1980).
13. A. H. Fanney and S. T. Liu, "Comparison of Experimental and Computer-Predicted Performance of 6 Solar Domestic Hot Water Systems". *ASHRAE Trans.* **86,** 823–833 (1980).
14. A. H. Fanney and S. A. Klein, "Performance of Solar Domestic Hot Water Systems at the National Bureau of Standards–Measurements & Predictions". *ASME J. Solar Energy Engng* **105,** 311–321 (1983).
15. G. L. Morrison and C. M. Sapsford, "Long-Term Performance of Thermosyphon Solar Water Heaters". *Solar Energy* **30,** 341–350 (1983).
16. J. E. Braun and A. H. Fanney, "Design and Evaluation of Thermosyphon Solar Hot Water Heating System". Proceedings of the American Solar Energy Society Annual Conference, *Program in Solar Energy*, pp. 283, 288. Minneapolis, Minnesota (1983).
17. J. J. Mutch, "Residential Water Heating, Fuel Conservation, Economics and Public Policy". Rand Report R1498 (1974).
18. C. W. F. von Koppen *et al.*, "The Actual Benefits of Thermally Stratified Storage in a Small and a Medium Size Solar System". *Proceedings of the ISES*, Atlanta, Georgia (1979).
19. W. B. Veltkamp, "Thermal Stratification in Heat Storage", in *Thermal Storage of Solar Energy*, (Edited by C. denOuden), Vol. 2, p. 47. Martinus Nijhoff, The Hauge (1980).
20. O. Rademaker, "On the Dynamics of (Thermal Solar) Systems Using Stratified Storage," in *Thermal Storage of Solar Energy*, (Edited by C. den Ouden), Vol. 2, p. 6. Martinus Nijhoff, The Hague (1980).
21. L. F. Jesch and J. E. Braun, "Variable Volume Storage and Stratified Storage for Improved Water Heating Performance". *Solar Energy* **33,** 83–87 (1984).
22. R. L. Cole and F. O. Bellinger, "Natural Thermal Stratification in Tanks", Phase 1, Final Report No. ANL-82-5. Argonne National Laboratory, Illinois (1982).
23. M. D. Wuestling, J. A. Duffie, S. A. Klein and J. E. Braun, "Investigation of Promising Control Alternatives for Solar Water Heating Systems," Proceedings of the American Solar Energy Society Annual Conference, *Progress in Solar Energy*, pp. 229, 234. Minneapolis, Minnesota (1983).
24. C. L. Gupta and H. P. Garg, "System Design in Solar Water Heaters with Natural Circulation". *Solar Energy* **12,** 163 (1968).
25. P. I. Cooper and J. C. Lacey, "Evaluation of a Household Solar Water Heating System Rating Procedure Using a Reference System for Performance Comparison". *Solar Energy* **26,** 213 (1981).
26. J. P. Wilford, R. B. Lehman and P. I. Cooper, "The Cost Factors of Auxiliary Electricity Supply to Domestic Solar Water Heaters". CSIRO Australia, Division of Mechanical Engineering TR30 (1981).
27. W. E Buckles and S. A. Klein, "Analysis of Solar Domestic Hot Water Heaters". *Solar Energy* **25,** 417 (1980).